JOURNAL OF CATALYSIS **159,** 83–89 (1996)
ARTICLE NO. 0066

Effect of Structure and Composition on Epoxidation of Hexene Catalyzed by Microporous and Mesoporous Ti–Si Mixed Oxides

Zhufang Liu, Gretchen M. Crumbaugh, and Robert J. Davis[1]

Department of Chemical Engineering, University of Virginia, Charlottesville, Virginia 22903-2442

Received June 28, 1995; revised October 9, 1995

A series of microporous titania–silica mixed oxides were characterized and tested as catalysts for the liquid-phase epoxidation of 1-hexene with *t*-butyl hydroperoxide. Results from ^{29}Si MAS NMR spectroscopy verified results from earlier characterization studies that indicated cohydrolysis of alkoxide precursors produced well-mixed oxide samples. The catalytic activity of the samples for hexene epoxidation at 353 K increased with increasing silica content. Since the fraction of tetrahedral Ti atoms in the samples also increased with silica content, the active site for the reaction is proposed to be a tetrahedrally coordinated Ti atom in a silica matrix. Polar solvents like water, acetone, and methanol inhibited the epoxidation reaction. To investigate the effect of pore size on activity, mesoporous Ti–Si mixed oxides analogous to MCM-41 were synthesized. The mesoporous samples were the most active and selective catalysts for epoxidation with TBHP, presumably due to the ease of access of the reactants to the active Ti sites. Results from EXAFS and UV reflectance spectroscopy indicated that Ti atoms in the mesoporous mixed oxides are tetrahedrally coordinated to oxygen atoms with the same Ti–O bond distance as TS-1. However, the activities of our mesoporous samples are orders of magnitude lower than that of TS-1 for hexene epoxidation with aqueous hydrogen peroxide. Lower hydrophobicity of a silica mesopore (2–4 nm) compared to a TS-1 micropore (0.6 nm) may account for the difference in activity observed in reactions with aqueous hydrogen peroxide.

INTRODUCTION

Catalytic oxidation processes are important in the production of commodity and fine chemicals. Heterogeneous catalysts such as silica-supported titania and titania–silica mixed oxides are known to be effective for selective oxidation reactions using organic hydroperoxides as the oxygen source (1). The discovery of Ti-substituted silicalite molecular sieve, TS-1, as a catalyst for selective oxidation reactions with aqueous hydrogen peroxide (2) was interesting since water is detrimental to conventional titania-based catalysts and no environmentally undesirable side products are formed from hydrogen peroxide reactions. It is generally believed that Ti atoms substitute isomorphously for Si in the molecular sieve framework of TS-1 to form the active oxidation site (3). The hydrophobic micropores of TS-1 (~0.6 nm in diameter) are proposed to screen out water from its internal voids thus protecting the Ti site from deactivation by water (4). However, the small size of the pores restricts the use of TS-1 to reactions involving small molecules. Recently, Ti-substituted Zeolite β was shown to be active for selective oxidation reactions with aqueous hydrogen peroxide (5, 6). Structural studies indicate that the local environment around Ti is similar in both TS-1 and Ti-β (7, 8) even though the wider micropores of Zeolite β (~0.7 nm) allow bulkier molecules to enter the zeolite voids and react (5, 6). There is continuing interest in the synthesis of catalysts with even larger pore sizes in order to accomodate bulkier molecules of importance for the production of fine chemicals. In this work, we compare the reactivity of microporous and mesoporous titania-silica mixed oxides for epoxidation of 1-hexene with both *t*-butyl hydroperoxide and aqueous hydrogen peroxide.

EXPERIMENTAL METHODS

The microporous Ti–Si mixed oxides were prepared by cohydrolysis of titanium isopropoxide and tetraethyl orthosilicate. These samples are the same as those used in earlier studies (9, 10). We also prepared mesoporous Ti–Si mixed oxides by the direct synthesis method of Corma *et al.* (11). The procedure is similar to the one used for preparing MCM-41 mesoporous silicas (12) but includes a titanium source in the synthesis mixture. A surfactant, either hexadecyltrimethylammonium chloride (Phaltz & Bauer) or decyltrimethylammonium bromide (Phaltz & Bauer), was first combined with an ammonium hydroxide solution. In a separate flask, tetramethylammonium hydroxide (Aldrich) was added to a 10 wt% solution of tetramethylammonium silicate (Sachem). After the two mixtures were combined, fumed silica (Cab-O-Sil M-5) was added while stirring. Finally, titanium ethoxide (Alfa) was added dropwise under stirring to produce a synthesis gel with a nominal loading of 2 mol% Ti. Gels were produced with compositions

[1] To whom correspondence should be addressed.

0021-9517/96 $18.00

$SiO_2 \cdot 0.020TiO_2 \cdot 0.085(C_{16}TMA)_2O \cdot 0.210(NH_4)_2O \cdot 0.263(TMA)_2O \cdot 29.93H_2O$ for the sample designated meso-TiSi-40 and $SiO_2 \cdot 0.017TiO_2 \cdot 0.092(C_{10}TMA)_2O \cdot 0.111(NH_4)_2O \cdot 0.259(TMA)_2O \cdot 28.72H_2O$ for the sample designated meso-TiSi-20. The synthesis gels were placed in Teflon-lines autoclaves and heated to 413 K for 28 h. The resulting solids were filtered, washed, and dried before they were calcined in flowing air at 813 K for 10 h. The designations meso-TiSi-40 and meso-TiSi-20 represent mesoporous titania–silica mixed oxides synthesized with surfactants that have been shown to form regular cylindrical pores with diameters of about 40 and 20 Å, respectively.

Dinitrogen adsorption isotherms were collected on a Coulter Omnisorp 100CX and a Micromeritics AccuSorb 2100 instrument. A Beckman DU-7 spectrophotometer equipped with a Labsphere, Inc. RSA BE-70 reflectance accessory was used to record the ultraviolet reflectance spectra of powder samples in air. Normalized absorption spectra were derived from the reflectance data according to the Kubelka–Munk formalism (13) using a Labsphere, Inc. SRS-99-010 white reflectance standard.

The microporous Ti–Si mixed oxides have been previously characterized by EXAFS, XANES, UV, Raman, and IR spectroscopies (9). Thus, the only additional structural characterization of these materials reported here involves ^{29}Si NMR spectroscopy. The ^{29}Si NMR spectra of pure silica and Ti–Si oxides were collected on a Bruker MSL 400 NMR spectrometer. The spinning rate, pulse width, and delay time were 3.8 kHz, 4 μs, and 6 s, respectively. The number of scans for collecting the single-pulse spectra was between 2000 and 10,000 depending on the Si loading of the sample. The cross-polarization–magic angle spinning spectra were recorded by using a contact time of 5 ms and a recycle delay of 4 s. All chemical shifts are reported relative to tetramethyl silane.

We also analyzed meso-TiSi-20 mixed oxide by X-ray absorption spectroscopy. The experiment was performed on beam line X18B at the National Synchrotron Light Source, Brookhaven National Laboratory (Upton, NY) in the transmission mode of data collection. The storage ring operated with an electron energy of 2.5 GeV with beam currents ranging from 100 to 200 mA. Higher harmonics in the beam were rejected by detuning the Si(220) monochromator crystals to 50% of the maximum intensity. The sample consisted of mixed oxide powder compressed between two Kapton windows. Thus, the X-ray spectrum is obtained for a catalyst at room temperature in air. As an energy calibration standard, a 4-μm-thick Ti foil (Goodfellow) was placed between the second and third ionization chambers, all of which were filled with a He/N_2 mixture to optimize sensitivity. The EXAFS data were processed with Macintosh versions of the University of Washington analysis programs. Anatase powder (Aldrich, 99.9%) was used as the reference material for structural information (interatomic distance, R; coordination number, N; and change in Debye–Waller factor, $\Delta\sigma^2$). An average distance of 1.95 Å was assigned to the Ti–O distance in anatase and the change in the Debye–Waller factor is reported relative to anatase at room temperature. Curve fitting was performed in the k-space region 3.3–9.1 $Å^{-1}$.

The epoxidation of 1-hexene by *t*-butyl hydroperoxide (TBHP) was typically carried out for 4 h at 353 K in a Teflon-lined Parr reactor using 50 mg of mixed oxide catalyst, 48 mmol of 1-hexene (Aldrich), and 4.8 mmol of anhydrous TBHP in decane (5–6 *M*, Aldrich). The product composition was determined by gas chromatography with nonane added as an external standard. Runs with aqueous hydrogen peroxide as an oxidant for the epoxidation were also examined. A 50-mg sample of catalyst was added to 6.26 g methanol, 0.66 g 1-hexene, and 0.18 g aqueous hydrogen peroxide (50% H_2O_2) at 323 K and stirred for 2 h. Epoxide concentration was determined by gas chromatography and peroxide concentration was determined by a cerium titration technique (14). For comparison, a TS-1 sample with a Ti/(Si + Ti) ratio of 0.024 was also tested as a catalyst for epoxidation with hydrogen peroxide. Detailed characterization of this TS-1 sample can be found in an earlier paper (8).

RESULTS AND DISCUSSION

A summary of the compositions and surface areas of the samples is presented in Table 1. Analysis of the *t*-plots derived from the dinitrogen adsorption isotherms indicated that samples prepared by cohydrolysis were microporous whereas samples prepared by liquid crystal templating were mesoporous. Micropores in the cohydrolyzed samples ranged from 1 to 1.5 nm in diameter as determined from the MP method. A full analysis of the porosity of the samples can be found in Ref. (15). The isotherms in Fig. 1 for meso-TiSi-40 and meso-TiSi-20 are similar to those reported previously for MCM-41 type materials (16, 17). The onset of capillary condensation occurs at higher relative pressures for meso-TiSi-40 compared to meso-TiSi-20,

TABLE 1

Surface Areas and Elemental Compositions of the Samples

Sample	Surface area ($m^2\ g^{-1}$)	Ti/(Ti + Si)
TiO_2	101	1
Ti : Si 6 : 1	310	0.85
Ti : Si 1 : 1	450	0.48
Ti : Si 1 : 8	410	0.11
Meso-TiSi-40	1052	0.020
Meso-TiSi-20	1051	0.015
SiO_2	380	0

TABLE 2

Results from Deconvolution of Single-Pulse ^{29}Si MAS NMR Spectra

	Q^4		Q^3		Q^2		Q^1	
Sample	ppm	%	ppm	%	ppm	%	ppm	%
SiO_2	−109.2	81.84	−99.8	14.62	−91.7	3.54		
Ti : Si 1 : 8	−109.7	61.39	−100.4	32.03	−91.4	6.58		
Ti : Si 1 : 1	−109.3	51.15	−100.2	33.82	−91.1	12.07	−83.1	2.96
Ti : Si 6 : 1	−109.0	21.02	−99.8	45.87	−90.3	28.53	−80.3	4.58

which is expected from the size of the templating molecules used in their synthesis.

Figures 2 and 3 show the ^{29}Si single-pulse (SP) and ^{1}H–^{29}Si cross-polarization (CP) solid-state MAS NMR spectra with peak deconvolution and curve fitting for pure silica and microporous Ti–Si mixed oxides. The SP SiO_2 spectrum clearly exhibits three well-resolved Gaussian peaks at chemical shifts of −109.2, −99.8, and −91.7 ppm, which can be assigned to Q^4[Si(SiO)$_4$], Q^3[Si(SiO)$_3$(OH)], and Q^2[Si(SiO)$_2$(OH)$_2$] structural units, respectively (18). The relative amounts of these different structural sites are derived from the integrated areas of the single pulse peaks and are reported in Table 2. As Fig. 2 shows, Q^4 sites are dominant in pure silica, indicating that the silica has a well-developed three-dimensional framework. About 19% of the Si nuclei are directly bonded to hydroxyl groups, which is consistent with the enhancement of the Q^3 and Q^2 signals relative to Q^4 under the CP condition. Previous work on silica gels and silicates has shown that the most likely

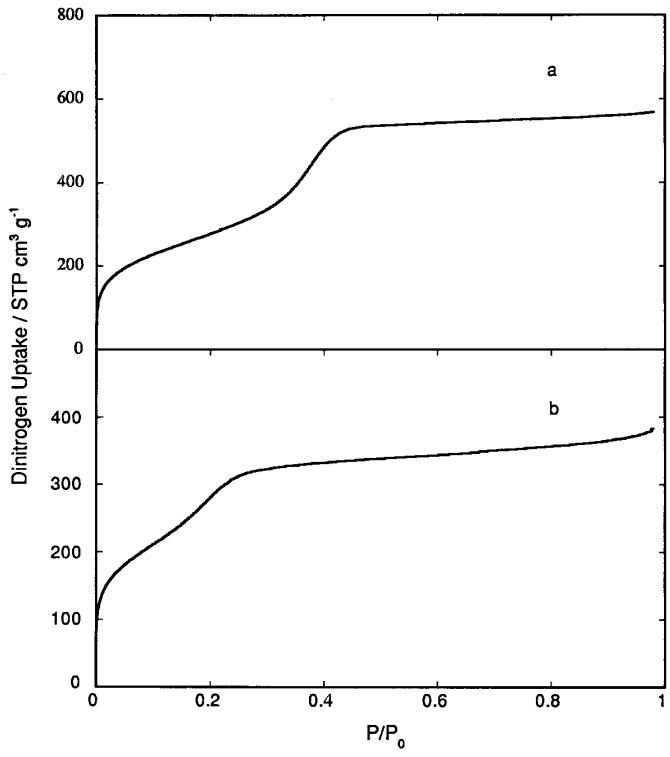

FIG. 1. Dinitrogen adsorption isotherms for meso-TiSi-40 (a) and meso-TiSi-20 (b) at 77 K.

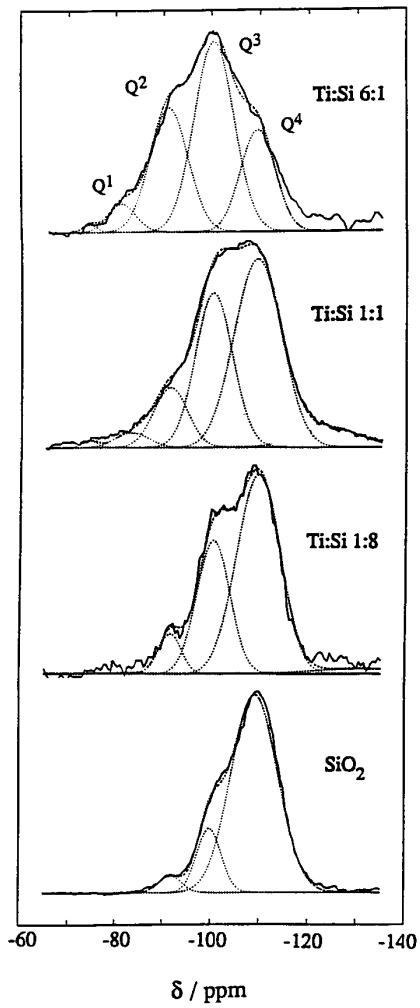

FIG. 2. ^{29}Si single-pulse MAS NMR spectra with peak deconvolution and curve fitting (dotted line) for pure silica and microporous Ti–Si mixed oxides.

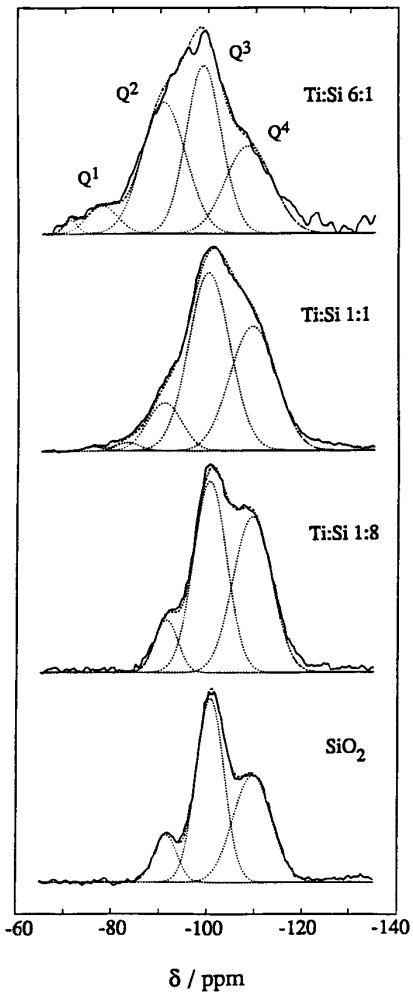

FIG. 3. ^{1}H–^{29}Si cross-polarization MAS NMR spectra with peak deconvolution and curve fitting (dotted line) for pure silica and microporous Ti–Si mixed oxides.

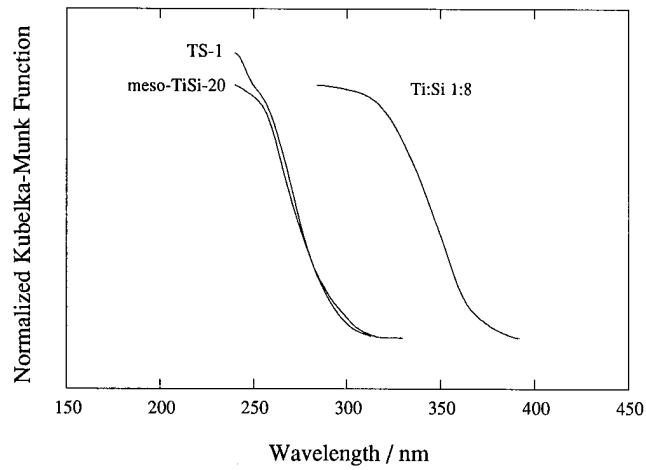

FIG. 4. Normalized absorption spectra derived from UV diffuse reflectance spectroscopy of meso-TiSi-20, TS-1, Ti : Si 1 : 8 in air.

candidates for ^{1}H–^{29}Si cross polarization are hydrogens in SiOH groups (18, 19), even though the hydrogens of adsorbed water could contribute to the enhancement under certain conditions. The spectra of Ti : Si 1 : 8 exhibit features similar to those of the synthesized silica, as shown in Figs. 2 and 3. However, the relative amount of Q^4 sites decreased, while Q^3 and Q^2 sites increased. Walther *et al.* also observed similar features in their study of mixed oxides (20). As silica was chemically mixed with titania, the three-dimensional framework of silica and the microstructure surrounding the silicon atoms were significantly perturbed by Ti atoms. However, care must be exercised when discussing the effect of Ti on the spectrum. After studying the ternary silicate glass SiO_2–TiO_2–ZrO_2, Wiles *et al.* found that –OH and –OTi groups have a similar influence on the chemical shift of the central Si atoms (21), which complicates the interpretation of the spectrum. This problem can be circumvented by comparing both the single-pulse and cross-polarized spectra of the Ti–Si mixed oxides with those of the pure silica. As shown in Fig. 2, the amounts of Q^3 and Q^2 increase with increasing Ti content. If the only non-Si atoms in the Q^3 and Q^2 groups were H atoms, then the signals for these groups in the spectra of the mixed oxides would be enhanced by the ^{1}H–^{29}Si CP procedure in a similar manner as silica. Instead, as a comparison of Figs. 2 and 3 indicates, the enhancement factors for the intensities of the Q^3 and Q^2 sites of the spectra of the mixed oxides are much less than those for the silica. Therefore, H atoms are not the only non-Si atoms in the Q^3 and Q^2 in the mixed oxides. Evidently, some Si atoms in the second shell were replaced by Ti atoms, indicating that Si–O–Ti bonds were generated upon the chemical mixing. This finding is completely consistent with earlier structural studies on these materials that utilized X-ray, UV, and IR spectroscopies (9).

The UV reflectance spectra in Fig. 4 indicate that Ti atoms in meso-TiSi-20 are similar to those in TS-1 since the absorption edges overlap. The absorption edge for meso-TiSi-40 (not shown) also coincides with the edge for TS-1. The large red shift of the absorption edge for Ti : Si 1 : 8 indicates that the Ti atoms are not completely isolated in the silica but exist in small microdomains with Ti–O–Ti linkages (9). The important result here is that Ti atoms in the mesoporous materials appear to be well isolated and may be tetrahedrally coordinated like the Ti atoms in TS-1.

Additional structural information in the vicinity of Ti in meso-TiSi-20 was derived from the Ti *K*-edge EXAFS shown in Fig. 5. Curve-fitting results in the following structural parameters: $R_{\text{Ti-O}} = 1.79$ Å, $N = 7.5$, and $\Delta\sigma^2 = -0.0054$ Å^2. Due to the large shift in inner potential (13 eV) needed to minimize the error of the curve fit and the narrow range of data used, we estimate that the interatomic distance is reliable to within 0.03 Å. The Ti–O interatomic distance for tetrahedrally coordinated Ti atoms in TS-1 is

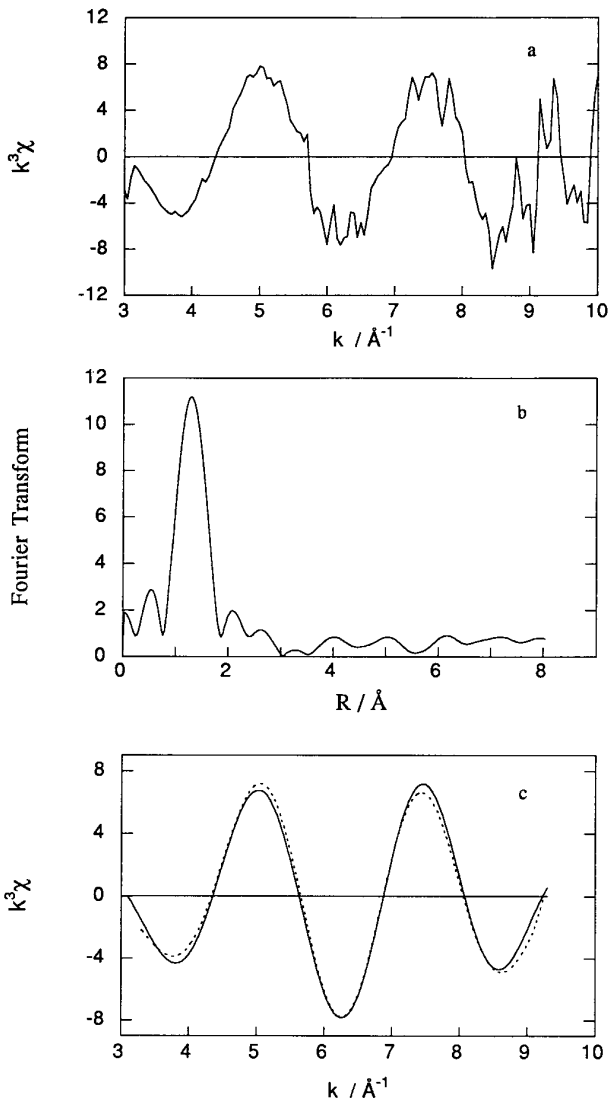

FIG. 5. Ti *K*-edge EXAFS for meso-TiSi-20. (a) $k^3\chi(k)$ data; (b) radial structure function derived from Fourier transform of data shown in (a), not corrected for phase shift; (c) Fourier-filtered EXAFS function and resulting curve fit (dotted line) used to calculate structural parameters.

1.80 Å (8), which compares very well with the distance measured in our mesoporous sample. The errors in the coordination number and change in Debye–Waller factor are known to be large for these materials (9), especially in light of the small wavevector range used for curve fitting, and we do not draw any conclusions from those parameters. However, the negative value of $\Delta\sigma^2$ is consistent with Ti atoms residing in a rigid silica lattice and having a short Ti–O bond distance (9).

Results for the epoxidation of 1-hexene with TBHP on Ti–Si mixed oxide catalysts are summarized in Table 3. The TBHP efficiency is defined as the percentage of 1,2-epoxyhexane produced compared to TBHP consumed. No epoxide was formed in the reactor without a catalyst. As expected, pure titania exhibited very low catalytic activity for the reaction. The observation that titania catalyzes the reaction was expected on the basis of the findings of Hutter *et al.* that pure titania catalyzed epoxidation of cyclohexene by cumene hydroperoxide (22). The activity and selectivity of our Ti–Si mixed oxide catalysts were higher than pure titania, but depended strongly on the composition. The most active and selective catalysts were the mesoporous mixed oxides that contained very little Ti. Of the microporous samples, Ti : Si 1 : 8 was the most effective catalyst for epoxidation.

An atomic structure of the highly active sites in the Ti–Si mixed oxides for the epoxidation reaction can be proposed on the basis of our extensive structural investigation of the mixed oxides (9) and earlier work on TS-1 (3). X-ray absorption spectroscopy of the Ti–Si mixed oxides has revealed that at least 70% of Ti atoms in the 1 : 8 sample reside in tetrahedral sites formed by direct substitution into silica (9). In addition, ^{29}Si NMR spectroscopy confirmed that Ti–O–Si bonds are formed in the dilute mixed oxides. The Ti sites for selective oxidation in TS-1 catalysts are known to contain tetrahedrally coordinated Ti atoms located in framework sites normally occupied by Si (3). Similarly, the highly effective catalytic sites for selective epoxidation on the Ti–Si mixed oxides are likely due to tetrahedral Ti atoms in a silica lattice, which is in agreement with the study of Imamura *et al.* (23). Hutter *et al.* propose that two types of sites exist on Ti–Si mixed oxides: one type associated with titania microdomains and a second type associated with isolated Ti, which is the highly active site (22). Our combined structure and reactivity results support their speculation.

The Ti : Si 1 : 8 sample exposes a significant fraction of its Ti atoms to the surface, as indicated by dramatic changes in the XANES at the Ti *K*-edge upon removal of ambient humidity (9). Thus, we expect far more tetrahedral Ti surface atoms on the Ti : Si 1 : 8 sample than on either of the very dilute mesoporous mixed oxides. However, meso-TiSi-40 converted more than twice the amount of TBHP to epoxide than microporous Ti : Si 1 : 8 under identical conditions. We

TABLE 3

Comparison of 1-Hexene Epoxidation Activity over Ti–Si Mixed Oxides[a]

Sample	TBHP conversion (%)	TBHP efficiency (%)
Blank	2.2	0
TiO_2	15.5	10.8
Ti : Si 6 : 1	34.7	20.8
Ti : Si 1 : 1	23.5	27.5
Ti : Si 1 : 8	37.6	77.2
Meso-TiSi-20	64.1	89.6
Meso-TiSi-40	86.4	84.1

[a] Conditions: 48 mmol 1-hexene, 4.8 mmol TBHP, 50 mg catalyst, 353 K, 4 h.

TABLE 4

Effect of Cosolvent on 1-Hexene Epoxidation[a]

Cosolvent	TBHP conversion (%)	TBHP efficiency (%)
Water	14.9	1.87
Methanol	29.9	7.5
Acetone	38.7	18.7
n-Butanol	17.9	68.8
Methy ethyl ketone	37.1	37.6
Decane	37.6	77.2
Isopropyl ether	27.2	79.5
1,1,2,2-Tetrachoroethane	40.1	76.7
2,4,6-tri-*t*-Butylphenol[b]	48.5	80.8

[a] Conditions: 48 mmol 1-hexene, 4.8 mmol TBHP, 50 mg Ti : Si 1 : 8 catalyst, volume ratio of decane to cosolvent = 2, 353 K, 4 h.

[b] Free radical inhibitor, 0.48 mmol added.

attribute the high activity of the mesoporous samples to the easy accessibility of the Ti sites to bulky reactant molecules like TBHP. Indeed, TBHP is completely unreactive in TS-1 molecular sieves which have micropores of about 0.6 nm (24).

We also studied the influence of cosolvents on 1-hexene epoxidation reaction catalyzed by Ti : Si 1 : 8 and the results are shown in Table 4. The reaction was greatly retarded by water, which is similar to the behavior of soluble metal catalysts (25). This finding can be attributed to the strong coordination of water with the surface of the mixed oxide, which blocks the active sites from reactant molecules. The presence of small alcohol and ketone compounds also decreased the selectivity of TBHP to epoxide product, but not to the same extent as added water. However, as less polar solvent molecules were added, the negative effect on epoxidation diminished. For example, isopropyl ether and 1,1,2,2-tetrachloroethane had little effect on the epoxidation reaction. Also, addition of a free radical inhibitor, 2,4,6-tri-*t*-butylphenol, to the reaction solution did not reduce the conversion or efficiency, implying that the epoxidation does not proceed through a radical mechanism in the liquid phase.

Earlier work indicated that mesoporous Ti–Si mixed oxide can catalyze selective epoxidation of 1-hexene with aqueous hydrogen peroxide (11). Table 5 compares the activity of our mesoporous materials to TS-1 for that reaction. Both mesoporous mixed oxides exhibited very low activity for 1-hexene epoxidation with 50% aqueous hydrogen peroxide. Similar results were observed when our microporous mixed oxides were used as catalysts for hexene epoxidation with aqueous hydrogen peroxide in acetone solvent. It is known that TS-1 and Ti-β show excellent activity and selectivity for epoxidation of olefins with aqueous hydrogen peroxide (5, 6), presumably because the small hydrophobic pores of molecular sieves effectively screen out water from

TABLE 5

Epoxidation of 1-Hexene with Aqueous Hydrogen Peroxide[a]

Sample	H_2O_2 conversion (%)	H_2O_2 efficiency (%)
TS-1	71.5	94.1
Meso-TiSi-40	23.7	1.4
Meso-TiSi-20	34.5	1.7

[a] Conditions: 6.26 g methanol, 0.66 g 1-hexene, 0.18 g aqueous H_2O_2 (50%), 50 mg catalyst, 323 K, 2 h.

the active Ti sites (4). In our case, both the microporous and mesoporous samples have average pore sizes greater than TS-1 and Ti-β. Apparently, the larger pores of our materials do not protect the active sites from inhibition by water.

The average rate of epoxidation over our mesoporous materials at 323 K is calculated from Table 5 to be 4×10^{-8} mol (g cat)$^{-1}$ s^{-1}, which is lower than the rate calculated from the data in Ref. (11) for the same reaction over a similar material but at lower peroxide concentration. From the data in that paper, we calculate the average rate of hexene epoxidation to be 2×10^{-7} mol (g cat)$^{-1}$ s^{-1} for Ti-MCM-41 at 329 K. However, the same laboratory reports that the initial rate of epoxidation over TS-1 is 13.5×10^{-6} mol (g cat)$^{-1}$ s^{-1} at similar temperatures and amounts of olefin and methanol (6), demonstrating that TS-1 is a much more active catalyst for the reaction. Although the hydrogen peroxide concentration was about a factor of four lower in the reaction with the mesoporous catalyst (6, 11), previous studies with TS-1 indicate that the order of reaction with respect to hydrogen peroxide varies between zero and first order, depending on concentration (24). Therefore, a factor of four difference in hydrogen peroxide concentration can not account for the factor of 68 difference in initial activity between TS-1 and mesoporous titanium silicate calculated from data in Refs. (6, 11). Thus, our current results confirm that TS-1 is a much more effective catalyst than mesoporous Ti–Si mixed oxide for selective epoxidation with aqueous hydrogen peroxide under identical conditions.

Even the minimal activity of the mesoporous materials for epoxidation in aqueous hydrogen peroxide solutions remains intriguing. Although, the mesoporous catalyst of Corma *et al.* (11) appears to be more active and selective than our mesoporous materials, this may result from a difference in experimental conditions. For example, we performed the reaction with an olefin/peroxide molar ratio of 3, which is five times lower than that used by Corma *et al.* (11). Since we used a relatively high concentration of peroxide, which implies a relatively high concentration of water, selective epoxidation activity is expected to be inhibited to a greater extent under our reaction conditions. In addition, the epoxidation reaction is likely to be affected by subtle variations in the materials as well as by the experimental conditions. As stated earlier, we believe that the

hydrophobicity of the silica structure in the vicinity of a Ti atom is very important for the reaction. Thus, the mesoporous channels of our catalysts could be less hydrophobic than those of Corma *et al.* due to a greater hydroxyl content. However, great differences in sample hydrophobicities are not expected since we treated our materials under similar conditions. Another speculation is that hydrophobic "pockets" may form in these samples and that Ti atoms in these pockets are active for epoxidation with aqueous hydrogen peroxide. The X-ray diffraction pattern of Ti-MCM-41 presented in Ref. (11) corresponds to a disordered array of mesoporous channels since higher-order peaks consistent with an ordered hexagonal array of cylinders were not observed. The difference between ordered and disordered mesoporous silicates has been fully documented by Davis *et al.* (26). Hydrophobic pockets may be located inside or between the silica channels in a disordered sample and their number density would certainly be extremely sensitive to the synthesis procedure.

CONCLUSIONS

Results from characterization of Ti–Si mixed oxides indicate that as the silica content is increased, the fraction of tetrahedral Ti atoms also increased. Catalytic activity for epoxidation of 1-hexene with *t*-butyl hydroperoxide over these materials was strongly correlated to the fraction of tetrahedral Ti atoms in the samples indicating that they are the active sites for the reaction. Mesoporous mixed oxides containing tetrahedral Ti were the most active catalysts for the epoxidation reaction with TBHP due to the ease of access of bulky reactants to the Ti sites. However, the same mesoporous mixed oxides were ineffective for the epoxidation reaction with aqueous hydrogen peroxide compared to titanosilicalite TS-1. Apparently, the hydrophobicity of a mesoporous sample is not adequate to screen out water from the active Ti site.

ACKNOWLEDGMENTS

Acknowledgments are made to the National Science Foundation for a Young Investigator Award (CTS-9257306) and to the donors of the Petroleum Research Fund, administered by the American Chemical Society (ACS-PRF 28260-AC5). R.J.D. also acknowledges support from a NATO travel grant to perform the NMR experiments in the laboratory of E. G. Derouane at the Facultés Universitaires Notre-Dame de la Paix, Namur, Belgium. We thank Guy Daelen for his help with collection of the NMR spectra. Research was carried out in part at the National Synchrotron Light Source, Brookhaven National Laboratory, which is supported by the U.S. Department of Energy, Division of Materials Sciences and Division of Chemical Sciences (DoE contract number DE-AC02-76CH00016).

REFERENCES

1. Wulff, H. P., and Wattimena, F., U.S. Patent 4 367 342 (1983).
2. Taramasso, M., Perego, G., and Notari, B., U.S. Patent 4 410 501 (1983).
3. Pei, S., Zajac, G. W., Kaduck, J. A., Faber, J., Boyanov, B. I., Duck, D., Fazzini, D., Morrison, T. I., and Yang, D. S., *Catal. Lett.* **21**, 333 (1993).
4. Khouw, C. B., Dartt, C. B., Labinger, J. A., and Davis, M. E., *J. Catal.* **149**, 195 (1994).
5. Corma, A., Camblor, M. A., Esteve, P., Martinez, A., and Perez-Parient, J., *J. Catal.* **145**, 151 (1994).
6. Corma, A., Esteve, P., Martinez, A., and Valencia, S., *J. Catal.* **152**, 18 (1995).
7. Blasco, T., Camblor, M. A., Corma, A., and Perez-Pariente, J., *J. Am. Chem. Soc.* **115**, 11806 (1993).
8. Davis, R. J., Liu, Z., Tabora, J., and Wieland, W. S., *Catal. Lett.* **34**, 101 (1995).
9. Liu, Z., and Davis, R. J., *J. Phys. Chem.* **98**, 1253 (1994).
10. Liu, Z., Tabora, J., and Davis, R. J., *J. Catal.* **149**, 117 (1994).
11. Corma, A., Navarro, M. T., and Pariente, J. P., *J. Chem. Soc. Commun.* **2**, 147 (1994).
12. Beck, J. S., Vartuli, J. C., Roth, W. J., Leonowicz, M. E., Kresge, C. T., Schmitt, K. D., Chu, C. T.-W., Olson, D. H., Sheppard, E. W., McCullen, S. B., Higgins, J. B., and Schlenker, J. L., *J. Am. Chem. Soc.* **114**, 10834 (1992).
13. Wenlandt, W. W., and Hecht, H., "Reflectance Spectroscopy," pp. 46–90. Wiley-Interscience, New York, 1966.
14. Schumb, W. C., Satterfield, C. N., and Wenworth, R. L., "Hydrogen Peroxide," p. 558. Reinhold, New York, 1955.
15. Liu, Z., Ph.D. dissertation, University of Virginia, 1995.
16. Tanev, P. T., Chibwe, M., and Pinnavaia, T. J., *Nature* **368**, 321 (1994).
17. Branton, P. J., Hall, P. G., and Sing, K. W. S., *J. Chem. Soc., Chem. Commun.* 1257 (1993).
18. Lippmaa, E., Magi, M., Samoson, A., Engelhardt, G., and Grimmer, A. R., *J. Am. Chem. Soc.* **102**, 4889 (1980).
19. Sindorf, D. W., and Maciel, G. E., *J. Am. Chem. Soc.* **105**, 1487 (1983).
20. Walther, K. L., Wokaun, A., Handy, B. E., and Baiker, A., *J. Non-Crystallogr. Solids* **134**, 47 (1991).
21. Wies, C., Meise-Gresch, K., Muller-Warmuth, Beier, W., Goktas, A. A., and Frischat, H. G., *Phys. Chem. Glasses* **31**, 138 (1990).
22. Hutter, R., Mallat, T., and Baiker, A., *J. Catal.* **153**, 177 (1995).
23. Imamura, S., Nakai, T., Kanai, H., and Ito, T., *J. Chem. Soc. Faraday Trans.* **91**, 1261 (1995).
24. Romano, U., Esposito, A., Maspero, F., Neri, C., and Clerici, M. G., *in* "New Developments in Selective Oxidation" (G. Centi and F. Trifiro, Eds.), p. 33. Elsevier, Amsterdam, 1990.
25. Sheldon, R. A., *J. Mol. Catal.* **7**, 107 (1980).
26. Davis, M. E., Chen, C.-Y., Burkett, S. L., and Lobo, R. F., *Mat. Res. Soc. Symp. Proc.* **346**, 831 (1994).